

Digital output silicon optical sensors

Oleksandr Malik*, F. Javier De la Hidalga-W, Carlos Zúñiga-I

*Electronics Department of the National Institute for Astrophysics, Optics, and Electronics (INAOE),
P.O. 51 and 216, Puebla, 72000, Mexico*

Received 28 September 2006; received in revised form 5 July 2007; accepted 7 August 2007
Available online 10 August 2007

Abstract

For the first time, a detailed description of low cost new intelligent (or smart) two-terminal optoelectronic devices without any on-chip circuitry for signal processing is presented. The design of the devices is based on the intelligent integration of micro-sized diodes and metal-oxide-semiconductor (MOS) capacitors. By combining physical processes and a functional voltage bias, such optical sensors transform the received analog input non-modulated optical signal directly into a pulse-width modulated electrical signal; the duty of the signal depends on the irradiation level, and the whole process is conducted without any integrated or external analog-to-digital converter. When the optical sensors operate under a pulsed irradiation synchronized with the functional voltage bias, unconventional logic properties are obtained that can be used to identify the emission from two equal LEDs.

© 2007 Elsevier B.V. All rights reserved.

Keywords: Silicon; Optical sensor; Intelligent sensor; Digital output

1. Introduction

Intelligent sensors, also known as smart sensors, usually are fabricated using the silicon technology as integrated circuits presenting both, transducer and electronic circuitry together on one silicon chip [1,2]. Due to the on-chip signal processing functions, such sensors can be connected directly with a microprocessor. This approach reduces the number of additional electronic components to a minimum, reduces the cost of the processing system, and improves the reliability. Successful realizations of such kind of sensors for optical and mechanical sensing are well known [3,4], as well as commercial sensors with on-chip signal processing, for instance, we can mention the optical sensor KPDC0028EA, from Hamamatsu Photonics Inc., with a light-to-frequency conversion, and the temperature sensor SMT 160-30, from Smartec, with a digital (pulse-width modulation) output.

Recently [5], we show that a light-to-frequency conversion can be obtained with two-terminal sensors designed by integrating in one chip micro-sized Schottky diodes (SDs), surrounded by metal-oxide-semiconductor (MOS) capacitors, with a com-

mon transparent electrode connecting in parallel these integrated structures.

In this work, we report for the first time a new two-terminal optical sensor presenting a digital output in the form of a pulse-width modulated (PWM) electrical signal. To obtain such digital output, analog-to-digital converters (ADC) were not necessary to be incorporated in the sensor's chip. It will be shown that when a functional voltage bias is applied to the sensor, the interrelation of the transport processes for the two sub-systems of carriers inside the device, namely electrons and holes, leads to the transformation of the input optical signal to the digital electrical signal at the output. This is a new approach for designing low cost digital output signal sensors. Furthermore, it will be also shown that our new sensors, through its "intelligence", allow for logic operations without the need of any additional electronic components.

2. Physical concept and design of the of new digital output sensors

The idea of these new sensors and the initial experimental results were reported for the first time some years ago [6,7]. However, only at this time, we are ready to discuss details of the physical processes occurring in this type of sensors as well as

* Corresponding author. Tel.: +52 222 247 05 17; fax: +52 222 247 05 17.
E-mail address: amalik@inaoep.mx (O. Malik).

their new characteristics and possible applications in optoelectronics.

To understand the idea of these new sensors, let us consider the cross-section of a simplified structure for the sensors as shown in Fig. 1. The structure contains a microscopic p-i-n diode surrounded by a MOS capacitor.

The microscopic p-i-n diode was fabricated on a high-resistivity π -type silicon substrate (1) by diffusion of boron through a small window opened in the silicon dioxide layer (2) for obtaining a p^+ micro-sized contact; a phosphorous dif-

fusion on the back side of the substrate was performed for obtaining an n^+ -contact (3). A common semi-transparent electrode (4) connects in parallel this microscopic $p^+-\pi-n^+$ diode with the surrounding MOS capacitor. The switch (S), is used to change the polarity of the voltage applied to the electrode. If the switch is in the position s1 (Fig. 1a), the positive voltage applied to the electrode originates two physical processes: a double injection of carriers from the n^+ and p^+ -contacts into the high-resistivity π -substrate, and the formation of an inversion layer at the silicon–silicon dioxide interface due to the accumulation of thermally generated electrons. The structure is in the ON state, and the current flowing in the circuit is determined by the applied voltage, the load resistor (R_L), and the series resistance of the $p^+-\pi-n^+$ diode. If at $t = t_0$, the switch is in position s2 during a short period of the time, the polarity of the voltage applied to the electrode will be changed (Fig. 1b), and new physical processes will take place. A space-charge region (SCR) is formed at the $\pi-n^+$ -contact. Electrons and holes are extracted from the substrate by the electric field of the SCR and through the p^+ -micro-contact, respectively. The structure is then in the OFF state, and the current in the circuit is determined by the reverse current of the diode. The functionality of these new sensors takes place when the switch returns to the position s1 (Fig. 1c). After that, the depletion regions appear at the silicon–silicon dioxide interface. These regions meet under the $p^+-\pi$ contact and the established potential barrier prevents the injection of holes from the p^+ -contact into the substrate. Without a source of holes, the electrons cannot be injected at the $n^+-\pi$ contact. Thus, even though the structure is forward biased, the current does not flow in the circuit and the device continues to be in the OFF state. The transition to the ON state takes a certain time that is necessary for the accumulation of thermally generated electrons in the potential well at the silicon–silicon dioxide interface in order to create an inversion layer. When this layer is formed, the wide of the SCR decreases [8]. The lateral widening of the SCR now is not enough to isolate the p^+ -contact, and a forward current (similar to that shown in Fig. 1a) starts flowing in the circuit. Thus, the structure returns to the ON state. In a general way, this proposed structure looks like the field-controlled thyristor reported in [9], in which the current voltage characteristics of micro-sized p-i-n diodes is controlled by the multiple grids obtained by diffusion of dopants into the silicon substrate. The potential applied to this grid determines the ON and OFF state of the device. The operating state of our structure, however, is determined also by the generation rate of minority carriers (electrons in Fig. 1) inside the silicon substrate. It is obvious that this time (the delay time) can be controlled by irradiating the structure. In practice, the batteries and the switch in the circuit shown in Fig. 1 can be implemented using the voltage from a functions generator (Fig. 1d).

In this work, 600 micro-sized ($20 \mu\text{m} \times 20 \mu\text{m}$) p^+ contacts, separated by $20 \mu\text{m}$ one from other, were fabricated at the top of a π -Si wafer ($\sim 10^{12} \text{ cm}^{-3}$) by boron diffusion in windows opened in the thermally grown SiO_2 layer. A uniform n^+ -contact was formed at the bottom of the silicon substrate by phosphorous diffusion. A common transparent conducting tin-doped indium oxide (ITO) electrode connects in parallel these

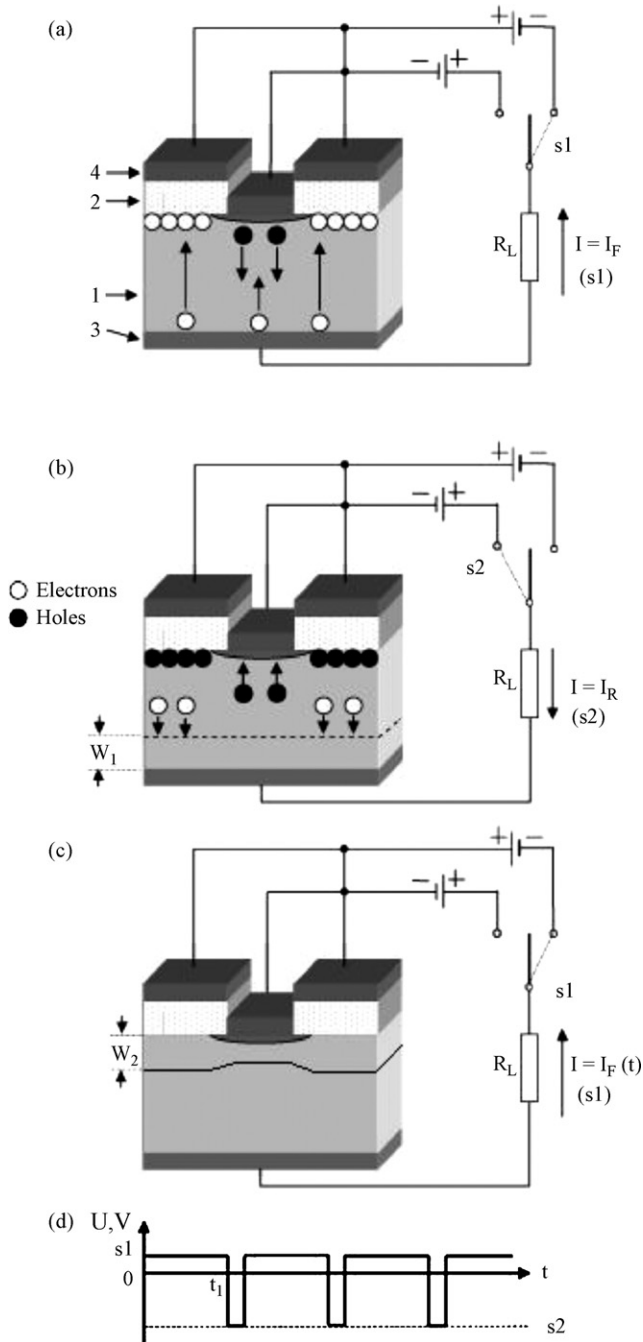


Fig. 1. Cross-section of a simplified structure for the sensor formed by a microscopic p-i-n diode surrounded by a MOS capacitor; they are connected in a circuit with two batteries, a switch, and a load resistor.

integrated structures. The forward current through the micro-sized $p^+-\pi-n^+$ junctions is controlled by the operating conditions of the surrounding MOS capacitors.

3. Experiment

3.1. Characteristics of the sensors obtained using a voltage ramp

Fig. 2 shows both non-irradiated and irradiated current-voltage (I - V) characteristics of the sensors obtained by applying a voltage ramp to the ITO electrode. The sensors were irradiated with a 930 nm wavelength near infra-red light-emitting diode (LED).

When the voltage ramp goes from a positive to a negative value, the I - V characteristics of the sensor for positive voltages is similar to that of a p - n diode. The forward current (I_1) does not depend on the irradiation level for a positive bias. For a negative voltage, the $p^+-\pi-n^+$ diodes are now reverse biased and the irradiation originates a photocurrent. When the voltage ramp goes from negative to a positive value, the forward current (I_2) is not the same under dark and irradiated conditions. Fig. 3 shows a zoom of the right part of Fig. 2.

Under dark conditions, when the generation rate of minority carriers is low, the filling of the potential well at the silicon-silicon dioxide forms an inversion layer and, as result, opens a “way” for carriers injection; this process takes a few milliseconds. That is the reason for the observed delay time of

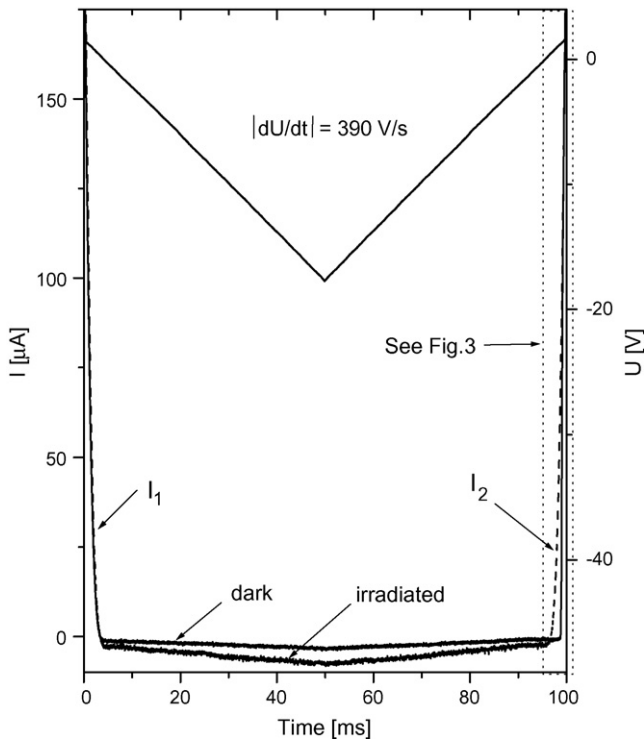


Fig. 2. The time-dependent I - V characteristics of the sensor under dark and irradiated conditions obtained by applying a voltage ramp (dU/dt) to the ITO electrode.

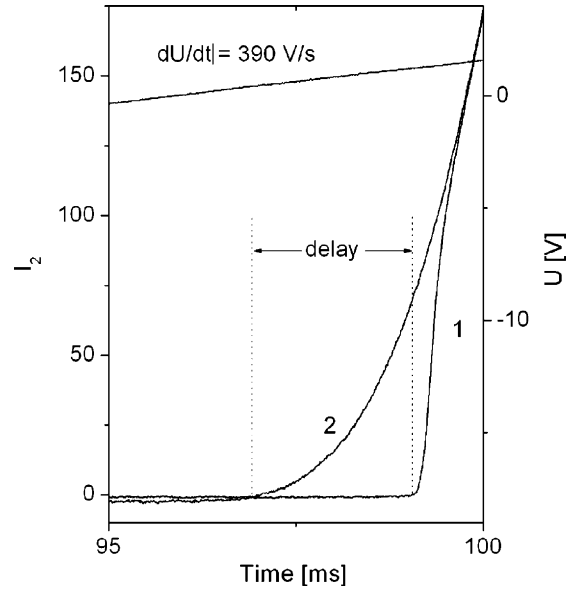


Fig. 3. Zoomed right side of Fig. 2 showing that the forward current I_2 obtained when increasing the voltage from negative to a positive value: 1 and 2—are the current under dark and irradiated condition, respectively.

the forward current increase (curve 1 in Fig. 3) in comparison with the current observed under irradiated conditions (curve 2 in Fig. 3), when the generation rate is significantly higher. The delay time depends on the irradiation intensity; a higher intensity leads to a shorter delay.

3.2. Characteristics of the sensors obtained with a pulse voltage

Further details of the physical processes occurring in the sensors and possible applications of the sensors were obtained from measurements in which the sensor is connected in series with a functions generator and a load resistor (R_L). The functions generator allows apply to the ITO electrode a constant positive voltage bias combined with a short negative pulse (Fig. 1d). The physical processes taken place under such conditions are shown schematically in Fig. 1.

When a positive constant voltage bias is applied to the ITO electrode (Fig. 1a), the MOS capacitors surrounding the $p^+-\pi-n^+$ diodes go to the inversion mode. The lateral spread of the depletion layer (W_f) is not enough to create the potential barrier for carriers below the p^+ -contacts, and a double injection (electrons from n^+ -contact and holes from p^+ micro-sized contacts) takes place. A comparatively high current, depending on the applied positive bias, flows in the circuit. When a short negative pulse is applied to the ITO electrode (Fig. 1b), minority and majority carriers are extracted from the π -type silicon substrate, and the SCR width is W_1 at the $\pi-n^+$ contact. When the voltage bias applied to the ITO electrode becomes again positive, the MOS capacitors surrounding the $p^+-\pi-n^+$ diodes go into the deep depletion mode (Fig. 1c), with a depletion width W_2 . The lateral spread of this width is enough to isolate the p^+ -contacts to inject holes into the silicon substrate. The structure does not return immediately to the state shown in Fig. 1a because the

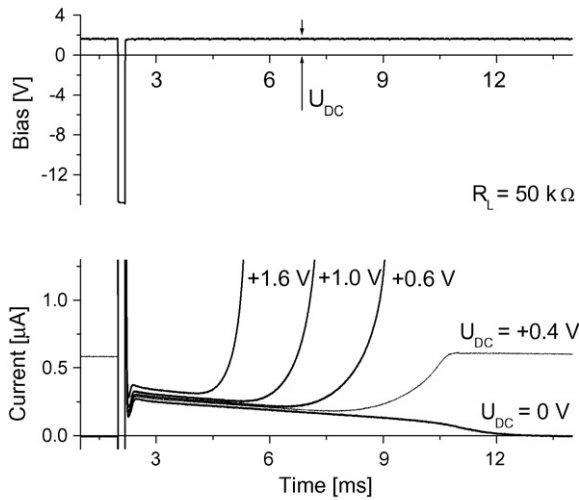


Fig. 4. The dependence of the delay time of the forward current increase after applying the negative pulse depends on the value of the applied positive DC bias. The value of the negative voltage pulse is the same (15 V).

reduction of W_1 is now a function of time due to the gradual accumulation of the electrons thermally generated in the silicon substrate into the potential well at the SiO_2 -silicon interface. When W_1 reduces to W_f , the potential barriers for holes below the p+ contacts disappear, and a high current due to a double carrier injection flows again in the circuit. Thus, after applying a short negative pulse, the structure returns to a conductive mode after some delay time (the time it takes the inversion layer to be formed at the SiO_2 -Si interface). This time depends on the voltage bias applied to the sensor and, also, on the irradiation intensity due to the carrier photo-generation inside the silicon substrate.

Fig. 4 shows how the delay in the forward current increase, after applying the negative voltage pulse, depends on the value of the applied positive DC bias.

For a fixed positive voltage bias, the irradiation of the sensors with the LED ($\lambda = 930 \text{ nm}$) reduces the time needed to obtain the ON state (Fig. 5), this is because of the increased generation rate of carriers inside the silicon substrate.

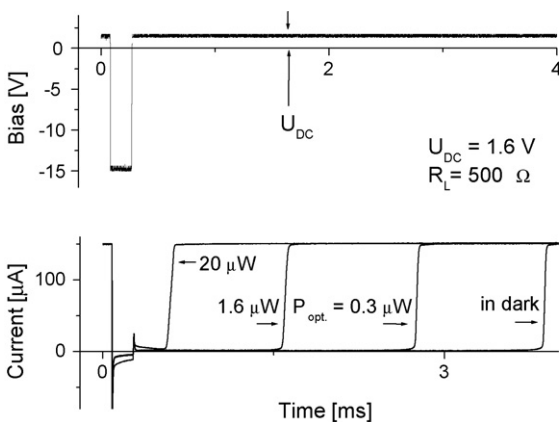


Fig. 5. Time dependence of the current in circuit under different irradiation levels (denoted as P_{opt}). The constant positive voltage bias (U_{DC}) applied to the ITO electrode is 1.6 V. The value of the negative voltage pulse is 15 V.

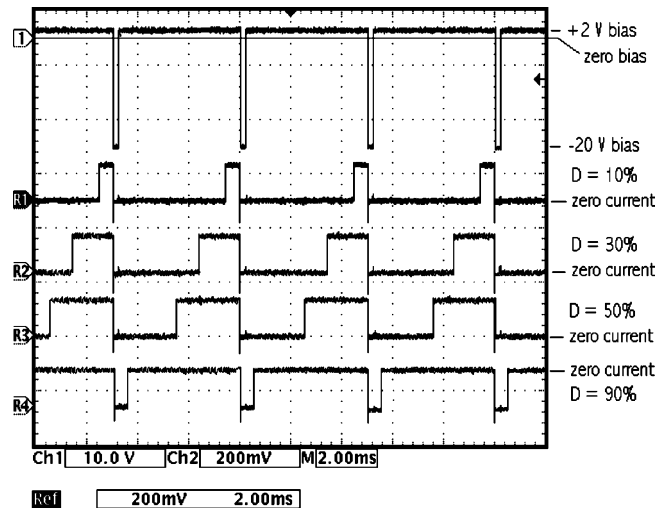


Fig. 6. The waveform of the applied voltage (at the top of the figure) and four oscillograms of the output signal obtained experimentally under dark and three different radiation intensities. The load resistor is $1 \text{ k}\Omega$ and the negative pulse repetition is 200 Hz. The zero levels of the functional voltage bias and current in the circuit are also shown.

3.3. Pulse-width modulated (PWM) output of the sensors under non-modulated irradiation

This type of digital output of the sensors could be obtained if the functional bias applied to the ITO electrode presents a periodical sequence of negative pulses in superposition with the DC bias as is shown in the upper part of Fig. 6. The four oscillograms shown below are the output signals of the sensor obtained experimentally under dark and irradiated conditions.

The duty (D) of the output signal is calculated as the ratio of the duration of the output pulse to the period of the negative pulses. The rise of the irradiation intensity reduces the delay time of the current increase after the negative pulse action, and increases the duty of the output signal. One can see how the duty of the output signal changes from 10% (under dark conditions)

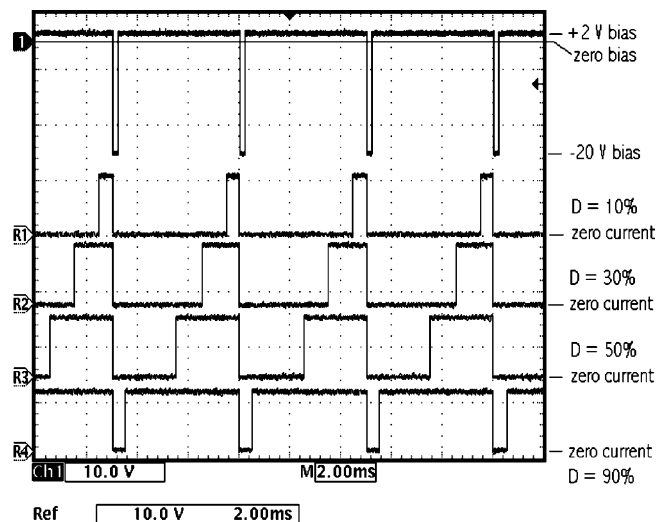


Fig. 7. The applied voltage bias (top oscillogram) and amplified output PWM signal (four lower oscillograms).

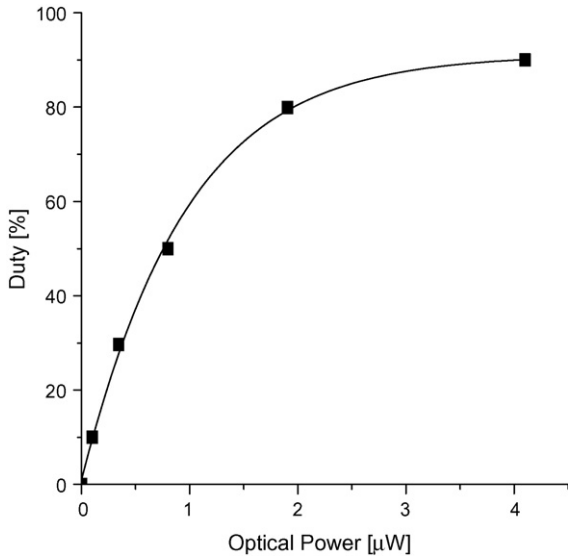


Fig. 8. Dependence of the duty on the incident optical power.

to 90% with the radiation intensity. The output signal presents a nearly rectangular waveform, which becomes more rectangular after a 60 dB amplification of the output signal up to 10 V (Fig. 7). The amplified negative pulses, due to the photocurrent flowing during the negative voltage pulses applied to the sensor, are suppressed by the diode in the measurement circuit.

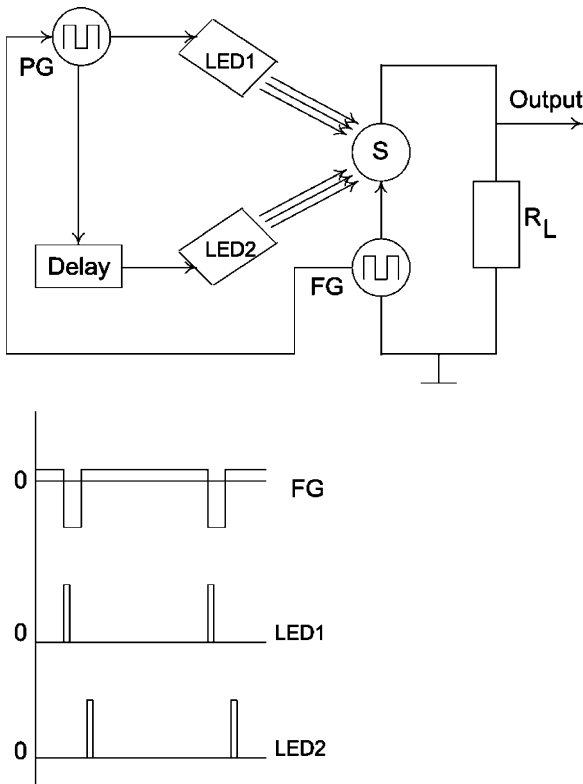


Fig. 9. Experimental setup used for the investigation of the PWM output of the sensor under a pulse irradiation. Here: S—sensor, FG—function generator, R_L —load resistor, LED1 and LED2—light emitting near infra-red diodes, PG—pulse generator, DELAY—delay line; the waveforms from the FG for biasing the sensor and the PG for pumping the LEDs are show below.

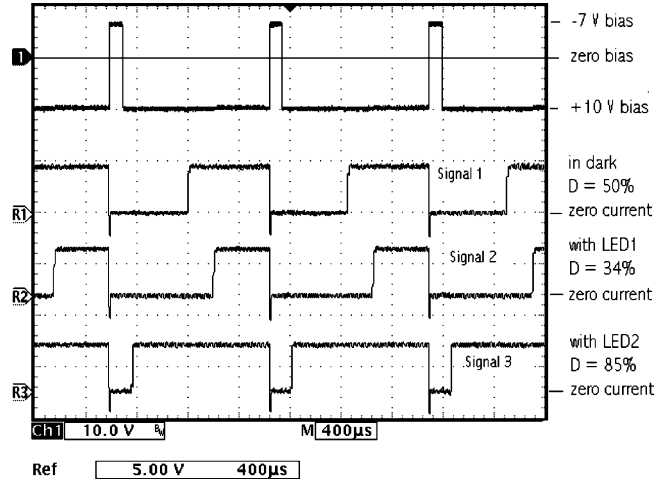


Fig. 10. Output PMW signal from the sensor under dark conditions and under illumination with LEDs synchronized at the leading (LED1) and trailing (LED2) edges of the negative voltage pulses applied to the ITO electrode. The voltage bias is shown inverse with respect to the previous figures. The negative pulse repetition is 800 Hz and the load resistor is 1 k Ω .

The dependence of the duty of the output signal on the incident optical power is shown in Fig. 8.

3.4. PWM output of the sensors under pulse irradiation

In this section we present some non-conventional properties of the sensors operating under pulse irradiation. The setup used for the measurements in this condition is shown schematically in Fig. 9.

The sensors were irradiated in turn with short pulses from two infra-red LEDs ($\lambda = 930$ nm). The pulse from the first one (LED1) was synchronized at the leading edge of the negative pulses applied to the ITO electrode. The second one (LED2) was synchronized at the trailing edge of these pulses. A constant positive voltage bias applied to the ITO electrode was chosen to obtain a 52% duty of the output PWM signal under dark

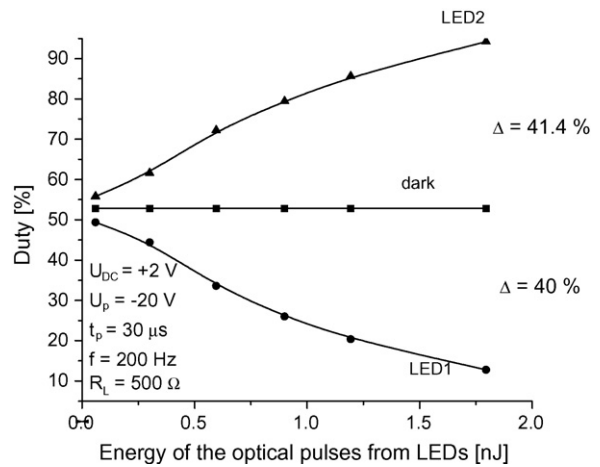


Fig. 11. Dependence of the duty of the PWM output signal on the energy of the optical pulses from LED1 and LED2. Here: U_{DC} and U_p —constant and pulse voltage applied to the sensor, t_p —duration of voltage pulse, f —the negative pulse repetition, R_L —load resistor, Δ —maximum variation of duty.

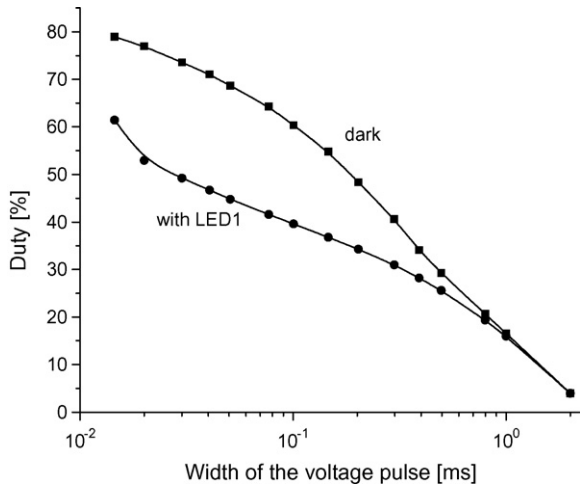


Fig. 12. Dependence of the duty of the PWM output signal on the width of the negative voltage pulse applied to the sensor for a pulse irradiation with LED1. The same dependence under dark condition is shown for comparison.

conditions. In Fig. 10 the output signal from the sensor is shown under dark and irradiation conditions from LED1 and LED2.

It is worth mentioning that the duty factor with LED1 and LED2 changes in different ways. With LED1, the duty factor decreases from 50 to 34%. However, with LED2, the duty factor increases up to 85%. This is obvious because of the enhanced generation of electron-hole pairs inside the silicon substrate under irradiation. Fig. 11 shows the dependence on energy of the optical pulses of the duty of the PMW output signal obtained experimentally under the conditions indicated in Fig. 11. The functional bias applied to the sensor was chosen in order to obtain a 52% duty of PMW output signal under dark condition.

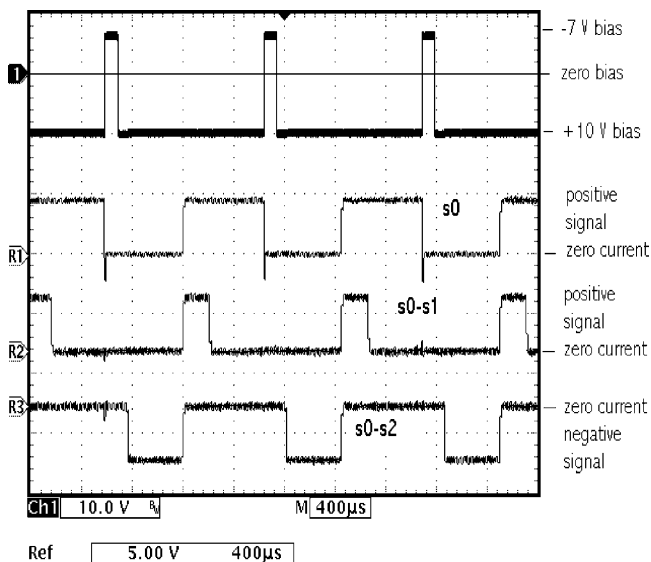


Fig. 13. Output signals obtained by subtracting the signals obtained with LED1 and LED2 (s_1 and s_2 , respectively) from the signal recorded under dark conditions (s_0). The energy from the $10 \mu\text{s}$ LED pulse is 4 nJ . The functional voltage bias is shown inverse with respect to Figs. 6 and 7. The negative pulse repetition is 200 Hz , and the load resistor is $1 \text{ k}\Omega$.

The variation of the duty on the width of the negative pulse bias for the sensor irradiated with LED1, relatively to the duty under dark conditions, only occurs if the voltage negative pulse-width does not exceeds 10^{-3} s (Fig. 12).

From Fig. 12 one can see that a pulse from LED1 is more efficient in changing the duty of the PWM output signal for a short negative voltage pulse applied to the sensor.

To understand the reduction of the duty factor under irradiation with LED1, further investigations need to be conducted. Nevertheless, the different response of the sensor to both LEDs, in other words, the ability of the sensor to identify two LEDs with the same emitted wavelength and power, can be useful for various technical applications, for instance, in robotics. Fig. 13 shows how two PWM output signals (s_1 and s_2) obtained with LED1 and LED2, respectively, are transformed by their simple subtraction from the output PMW signal (s_0) obtained under dark conditions.

One can see from Fig. 13 that the signals (s_0-s_1) and (s_0-s_2) present a different polarity in addition to a different duty factor.

4. Conclusions

The PWM electrical signal at the output of the sensors, which were described in detail in this work for the first time, is obtained without the need of integrating on the same silicon chip any additional signal converting electronic components.

It was shown that when a functional voltage bias is applied to the sensor, the interrelation of the transport processes for the electron and hole sub-systems, leads to the transformation of the analog optical signal at the input to the digital electric signal at the output.

Due to their digital output, these sensors were connected directly to a PIC16F877 microcontroller. This microcontroller, at the same time, was used as the source for the functional voltage bias necessary for operating the sensor.

The optical sensors described in this work operate under both modulated and non-modulated irradiation. Under a pulse irradiation, the sensors present some non-conventional properties that can be used to identify the emission from two equal LEDs. This principle can be used for the design of logic circuits to be applied in robotic and in automatic control.

Finally, a further detailed investigation of these proposed low cost devices, together with the simulation of the physical processes occurring inside them, will help for the optimization of their properties in order to improve their design for different useful optical, mechanical, and biomedical applications.

Acknowledgement

This work was partially supported by CONACyT-Mexico under grant 39886.

References

- [1] D. Dubey, Smart sensors, M. Tech. credit seminar report, Electronic Systems Group, EE Dept, IIT Bombay, November 2002.

- [2] S. Middelhoek, A.C. Hoogerwerf, Smart sensors: when and where? *Sens. Actuators* 8 (1985) 39–48.
- [3] G. de Graaf, R.F. Wolffenbuttel, Smart optical sensor systems in CMOS for measuring light intensity and colour, *Sens. Actuators A: Phys.* 67 (1998) 115–119.
- [4] F.R. Riedijk, T. Smith, J.H. Huijsing, An integrated optical position-sensitive detector with digital output and error correction, *Sens. Actuators A: Phys.* 40 (1994) 237–242.
- [5] O. Malik, V. Grimalsky, J. De la Hidalga-W, Behavior of an optical sensor based on non-ideal silicon capacitors: from amplification to generation, *Sens. Actuators A: Phys.* 130–131 (2006) 208–213.
- [6] O. Malik, R. Martins, Silicon active optical sensors: from functional photodetectors to smart sensors, *Sens. Actuators A: Phys.* 68 (1998) 359–364.
- [7] O. Malik, M. Aceves, Improved two-terminal silicon functional optical sensor, *Modern Phys. Lett. B* 15 (2001) 722–725.
- [8] S.M. Sze, *Physics of Semiconductor Devices*, Wiley, New York, 1981.
- [9] D.E. Houston, S. Krishna, D.E. Piccone, et al., A field terminated diode, *IEEE Trans. Electron. Devices* 23 (1976) 905–910.

Biographies

Oleksandr Malik received his M.Sc. degree in Optics and Ph.D. in Physics of Semiconductors and Dielectrics from the Chernivtsy University, Ukraine, in 1971 and 1980, respectively. He specialized in thin metal-oxide film technology and its applications used in optoelectronic devices during 36 years of scientific and industrial activity. From 1996 to 1999, he worked in Portugal as an invited scientist. Since 2000 he works as a titular researcher at National Institute for Astrophysics, Optics, and Electronics (INAOE), Electronics Department, Puebla, Mexico. His activity is connected with the development of new transparent conducting semiconductor films, novel optoelectronic devices, and solar

cells with their applications. O. Malik is an author of about 200 scientific papers. He is a Senior Member of IEEE.

F. Javier De la Hidalga-W received the B.Sc. degree in Electrical Engineering from Universidad Autónoma de Puebla, Puebla, Mexico, in 1992, and the M.Sc. and Ph.D. degrees in Electronics in 1994 and 1998, respectively, from Instituto Nacional de Astrofísica, Óptica y Electrónica (INAOE), Puebla, Mexico. He was a postdoctoral fellow in Simon Fraser University (SFU), Burnaby, B.C., Canada, and in McMaster University, Hamilton, Ontario, Canada, from 1998 to 1999. In 2001, he was also a visiting professor in McMaster University. Since 1999 he is a member of the research staff at the Electronic's Department of INAOE. He has co-authored three book chapters on low temperature semiconductor devices, published about 20 journal papers, and presented more than 30 international conferences. His current interest includes research on low temperature semiconductor devices and circuits for long wave length detectors, and modeling and characterization of deep submicron MOSFETs operating in the 4.2–350 K temperature range.

Carlos Zuñiga-I studied Electrical Engineering in the Instituto Politécnico Nacional (IPN), Mexico City, and obtained the Master and Ph.D. degrees in 1997 and 2005, respectively, from the National Institute for Astrophysics, Optics and Electronics (INAOE), Puebla, Mexico. Since 1982, he has worked at the Electronics Department of INAOE, giving technical support to the equipment and fabrication processes of devices and circuits, and has also participated in group, individual and independent projects. Currently, he is the head of the Microelectronics Laboratory and a full time researcher at INAOE. Among his fields of interest is the deposition of dielectric and semiconductor materials using Low Frequency Plasma Enhanced Chemical Vapor Deposition (PECVD). He has produced several scientific and technical contributions that have been published in book chapters and journal papers, as well as many presentations in conferences.